Hindawi
Advances in Civil Engineering
Volume 2019, Article ID 2612536, 9 pages
https://doi.org/10.1155/2019/2612536

Research Article

Experimental Investigation on the Axially Loaded Performance of Notched Hexagonal Concrete-Filled Steel Tube (CFST) Column

Jing Liu,[1,2] Zhe Li,[3] and Fa-Xing Ding[2]

[1]*School of Civil Engineering, Hunan City University, Yiyang, Hunan Province 413000, China*
[2]*School of Civil Engineering, Central South University, Changsha, Hunan Province 410075, China*
[3]*School of Architecture and Art, Central South University, Changsha, Hunan Province 410075, China*

Correspondence should be addressed to Zhe Li; lizhe88@csu.edu.cn and Fa-Xing Ding; dinfaxin@csu.edu.cn

Received 15 July 2019; Revised 24 August 2019; Accepted 1 September 2019; Published 29 September 2019

Academic Editor: Rosario Montuori

This study aimed to investigate the static performance of notched hexagonal concrete-filled steel tube (CFST) stub columns through axial loading. Notch length, notch location, and notch direction in 14 CFST stub columns were experimentally studied. Stress process, failure mechanism, and ultimate strength in the notched CFST columns were analyzed. Results show that notches in steel tubes can weaken the restraining effect of steel pipes on core concrete and induce a decrease in the ultimate strength of specimens. The failure mode of components is greatly affected by notch orientation. The notch is closed under axial compression in the horizontally notched specimen, and the slotting indicates outward buckling in the vertically notched specimen. Based on the test results, a method for calculating the ultimate strength of notched hexagonal CFST columns was established. This research encourages the extensive application of these structures in civil engineering.

1. Introduction

Concrete-filled steel tube columns are extensively used in engineering due to their simple joint structures, convenient connections, and excellent flexural behavior. CFST columns have been widely explored worldwide, and considerable progress has been made [1–5].

However, some CFST problems remain unsolved. Some damages weaken the mechanical properties of CFST columns, thereby affecting the structural integrity and reducing the working life of the columns. (1) As with other metal structures, initial geometric and material defects exist in the external steel pipes of CFST members, and CFST columns are inevitably affected by corrosion and other external loads upon use [1]. (2) In some engineering projects, such as those involving the connection of steel with a concrete composite beam and CFST column joints, notches must be cut onto the steel pipe. This method weakens the restraint effect of steel pipe on the core concrete at the joints. Consequently, the stiffness of the notched section decreases, adversely affecting the seismic performance of CFST columns at the joints [2–4].

These problems have been addressed in recent years. (1) Regarding the geometric and material defects of CFST columns, Nia et al. [6] investigated the influence of initial buckling on the mechanical performance of a square steel pipe under oblique loading. Sadovský et al. [7] investigated the effect of initial geometric imperfections on the buckling strength of steel members. Zhang et al. [8] studied the influence of initial buckling on the energy dissipation of steel pipes under axial compression. Nia et al. [9] assessed the energy absorption of a square pipe with a buckling initiator. (2) Chang et al. [10] and Ding et al. [11] carried out axial compression performance tests on circular or square CFST columns with defects. They then proposed the ultimate bearing capacity calculation formula, which is based on experimental data fitting, for such components. Liu and Young [12] studied the effect of buckling on steel square hollow section compression members and analyzed the strength of the test column with three different specifications. Han et al. [1] investigated the mechanical properties of square CFST columns under loading and chloride corrosion and then compared the ultimate strength of loaded CFST columns with different specifications. Chen et al. [13, 14] explored the axial compression property of CFST columns and considered the hole rate, concrete strength grade, and slenderness ratio. They subsequently proposed the calculation method of ultimate bearing capacity for damaged CFST columns. Ding et al. [15] investigated the composite action of notched circular CFST stub columns under axial compression through numerical and theoretical studies and then presented an empirical formula to predict their ultimate capacity.

In China, hexagonal CFST columns have been applied in the Gao Yin Finance Building in Tianjin and the CITIC Tower in Beijing [16], as shown in Figure 1. Studies on the effect of hexagonal CFST columns on static performance have mostly considered axial compression and bending [16–19]. Notched circular and rectangular CFST columns have been researched, but notched hexagonal CFST columns remain rarely studied.

The present work focused on the static performance of notched hexagonal CFST columns based on our team's previous research [11, 15, 17]. The objectives were as follows: (1) to experimentally study 14 CFST stub columns and their parameters, including notch length, notch location, and notch direction and (2) to establish a method for calculating the ultimate strength of notched hexagonal CFST stub columns.

2. Experimental Study

2.1. Introduction of Test. Twelve notched hexagonal CFST columns and two intact CFST columns were included in the experimental study. Notch length, notch location, and notch direction were considered and investigated. All specimens had the same section size, and the material performance of the steel and concrete cube was tested through standard method before the experiment. Table 1 shows the geometric properties and characteristics of the CFST columns, and Figure 2 presents a diagram of the notched hexagonal CFST specimens. In the equation, l and b are the length and width of the notch, respectively; D is the side of the hexagon cross section; t is the thickness of the steel pipe; H is the height of the specimen; f_s is the yield strength of the steel pipe; and f_{cu} is the compressive strength of the concrete cube.

2.2. Loading Scheme. The test adopted a 5000 kN press. Figure 3 shows the sketch of the test setup for the CFST stub column. The displacement-control loading system of the test comprised the following: the elastic stage, in which 1/15 of the bearing capacity load was increased per load, and the elastic-plastic stage, in which 1/25 of the ultimate load was increased per load. The load duration was approximately 3 min per level. Deformation data were collected with an electronic displacement meter. The CFST columns were constantly loaded until failure. The failure process and mode were observed, and displacement and ultimate load were recorded. Each specimen test lasted for approximately 2 h. According to the characteristics of this specimen, the test was interrupted when the axial displacement reached 0.035 H.

2.3. Loading Phenomenon. Figure 4 shows the failure modes for test specimens. The modes can be divided into two types. In the hexagonal CFST column with horizontal slotting, the notch was closed under axial loading, as shown in Figures 4(a) and 4(b). In the hexagonal CFST column with vertical slotting, the slotting showed outward buckling, as demonstrated in Figures 4(c) and 4(d).

The entire steel pipe was cut by the end of the experiment. Figure 5 shows the failure of the core concrete. (1) In the hexagonal CFST column with horizontal slotting, concrete crushing was observed near the notches, as shown in Figures 5(a) and 5(b). (2) In the hexagonal CFST column with vertical slotting, concrete breakage was severe. (3) The failure phenomenon of the notched specimen in the corner was more evident than that in the side.

2.4. Analysis of Test Results. Figure 6 shows the load-displacement curve of the specimens. The static tests of the CFST columns can be implemented in three stages: elastic, elastic-plastic, and failure stages.

2.4.1. Elastic Stage. The hexagonal CFST columns are in the elastic phase when their strength is 0.7 of the ultimate strength, and the load-displacement curve is closely linear.

2.4.2. Elastic-Plastic Stage. The axial displacement grows nonlinearly as the axial load achieves the yield load. The linearly increasing trend of axial displacement decreases with increasing load, showing a slow increasing trend. Buckling deformation does not appear in the steel pipe.

2.4.3. Failure Stage. The strength of CFST columns decreases when the load exceeds the limit strength. Moreover, deformation intensifies in the slotting of the specimens with increased axial deformation. Bearing capacity increases to some extent after the axial deformation of some specimens reaches approximately 0.025 H.

Figure 6 compares the load-axial deformation curves of the notched and intact specimens. The geometric and material parameters of the two specimens are the same. The stiffness of the two columns has no evident difference in the elastic stage. The peak load of the notched specimen is lower than that of the intact specimen because the notch induces the premature failure of the steel pipe and greatly weakens the restraint effect of the steel pipe on the concrete core.

3. Effects of Three Parameters on the Axial Compression Performance of Hexagonal CFST Column

3.1. Influence of Notch Length. Figure 7 illustrates the effects of slotting length on the mechanical properties of hexagonal

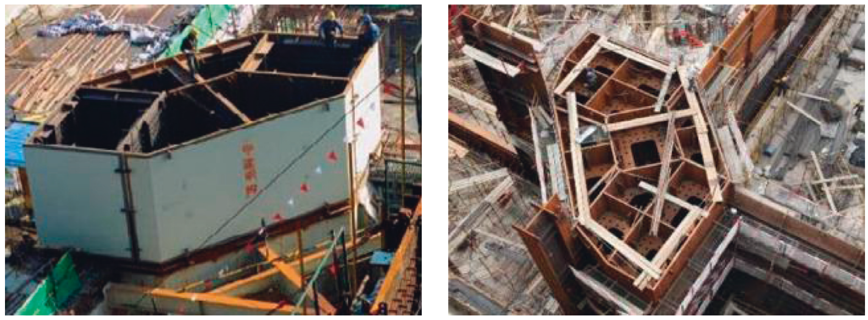

(a) (b)

Figure 1: Adhibition of hexagonal CFST columns in practical engineering projects. (a) Gao Yin finance building. (b) CITIC tower.

Table 1: Geometric properties and characteristics of CFST columns.

	No.	Orientation	Location	$l \times b$ (mm)	$D \times t \times H$ (mm)	f_s	f_{cu}	N_c	N_t
1	HCFT1	Horizontal	Sidewall	100×10	$100 \times 4 \times 600$	270	37.5	1468	1483
2	HCFT2	Horizontal	Sidewall	60×10	$100 \times 4 \times 600$	270	37.5	1502	1529
3	HCFT3	Horizontal	Sidewall	30×10	$100 \times 4 \times 600$	270	37.5	1527	1557
4	HCFT4	Horizontal	Corner	100×10	$100 \times 4 \times 600$	270	37.5	1488	1456
5	HCFT5	Horizontal	Corner	60×10	$100 \times 4 \times 600$	270	37.5	1514	1502
6	HCFT6	Horizontal	Corner	30×10	$100 \times 4 \times 600$	270	37.5	1534	1538
7	HCFT7	Vertical	Sidewall	100×10	$100 \times 4 \times 600$	270	37.5	1519	1530
8	HCFT8	Vertical	Sidewall	60×10	$100 \times 4 \times 600$	270	37.5	1530	1558
9	HCFT9	Vertical	Sidewall	30×10	$100 \times 4 \times 600$	270	37.5	1539	1574
10	HCFT10	Vertical	Corner	100×10	$100 \times 4 \times 600$	270	37.5	1527	1468
11	HCFT11	Vertical	Corner	60×10	$100 \times 4 \times 600$	270	37.5	1536	1516
12	HCFT12	Vertical	Corner	30×10	$100 \times 4 \times 600$	270	37.5	1542	1569
13	HCFT13	Unimpaired	—	—	$100 \times 4 \times 600$	270	37.5	1555	1579
14	HCFT14	Unimpaired	—	—	$100 \times 4 \times 600$	270	37.5	1555	1580

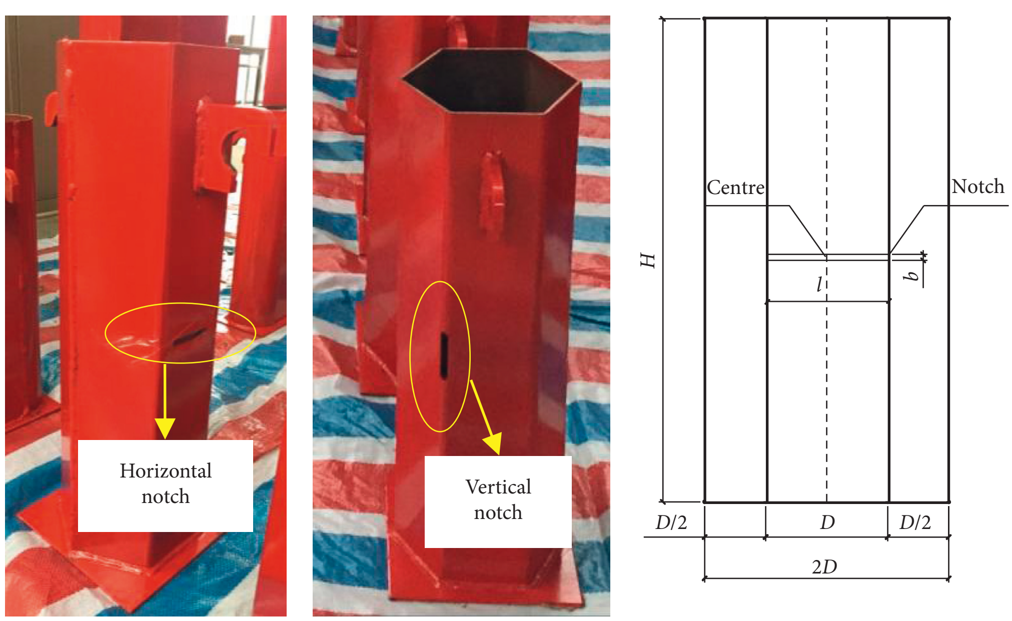

(a) (b) (c)

Figure 2: Diagram of notched hexagonal CFST specimens. (a) Horizontal slotting. (b) Vertical slotting. (c) Dimension diagram of a notched specimen.

(a) (b)

Figure 3: Sketch for testing the apparatus of CFST stub column. (a) Test setup. (b) Loading device.

(a) (b) (c) (d)

Figure 4: Failure modes for hexagonal CFST columns. (a) Horizontal notch in the sideway. (b) Notch in the corner. (c) Vertical notch in the sideway. (d) Vertical notch in the corner.

CFST stub columns. The notch lengths are 30, 60, and 100 mm. A long notch length leads to weak restraint effect and low ultimate strength of the specimen.

In the horizontally notched specimens, the carrying capacities of the specimens with a notch length of 30 mm are 2.1% and 5.3% larger than those of specimens with notch lengths of 60 and 100 mm, respectively. In the vertically notched specimens, the carrying capacities of specimens with a notch length of 30 mm are 2.2% and 4.8% larger than those of specimens with notch lengths of 60 and 100 mm, respectively.

3.2. Influence of Notch Location. Figure 8 illustrates the effects of slotting location on the mechanical performance of hexagonal CFST stub columns. The notches are located at the sideway and corner. Given the weak overall mechanical behavior of steel pipe and concrete in the corner, the ultimate strength of the CFST column notched in the corner is smaller than that in the sideway. In the horizontally notched specimens, the carrying capacities of the specimens with a sideway notch are 1.6% larger than those of specimens with a vertical notch. In the vertically notched specimens, the carrying capacity of the specimen with a sideway notch is 2.4% larger than those of specimens with a corner notch.

3.3. Influence of Notch Direction. Figure 9 presents the effects of slotting orientation on the work performance of hexagonal CFST stub columns. The notch orientations include horizontal and vertical. Given the weak overall mechanical behavior of steel pipe and concrete in the corner, the ultimate bearing capacity of the corner-notched specimens is smaller than that in the middle one. For sideway-notched

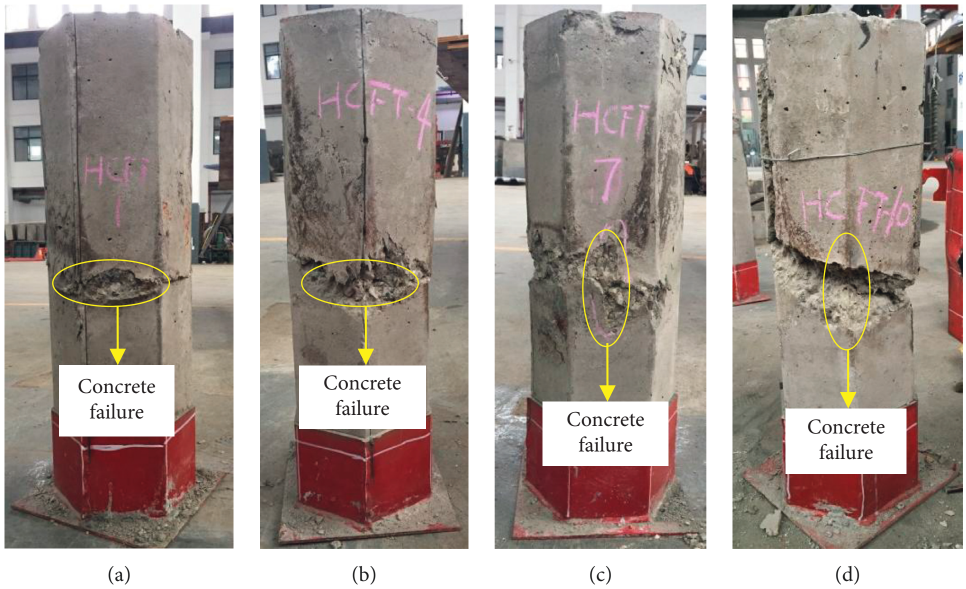

Figure 5: Core-concrete damage of typical specimens. (a) Horizontal slotting in the sideway. (b) Horizontal slotting in the corner. (c) Vertical slotting in the sideway. (d) Vertical slotting in the corner.

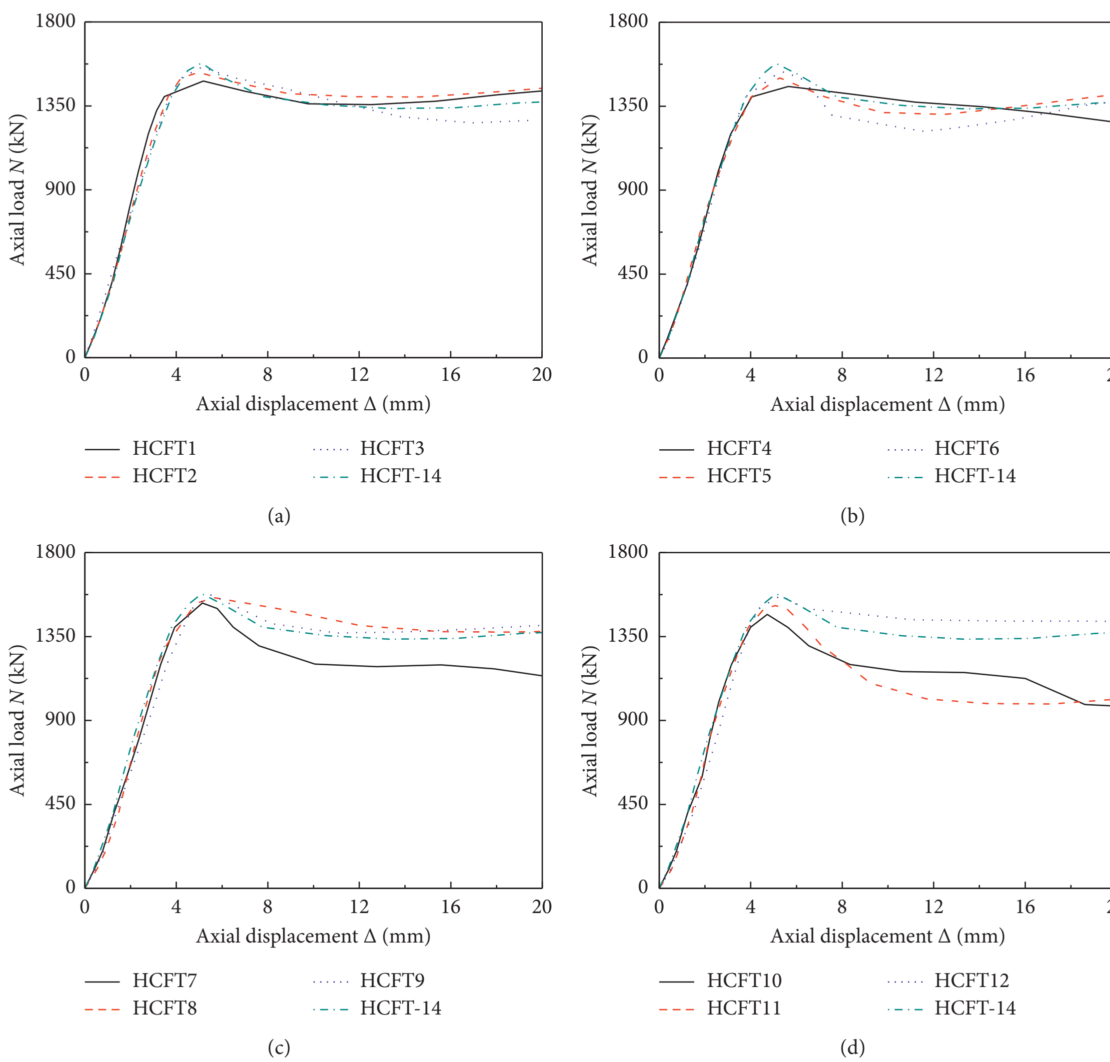

Figure 6: Load-displacement curve of hexagonal CFST columns. (a) HCFT1~HCFT3. (b) HCFT4~HCFT6. (c) HCFT1~HCFT3. (d) HCFT4~HCFT6.

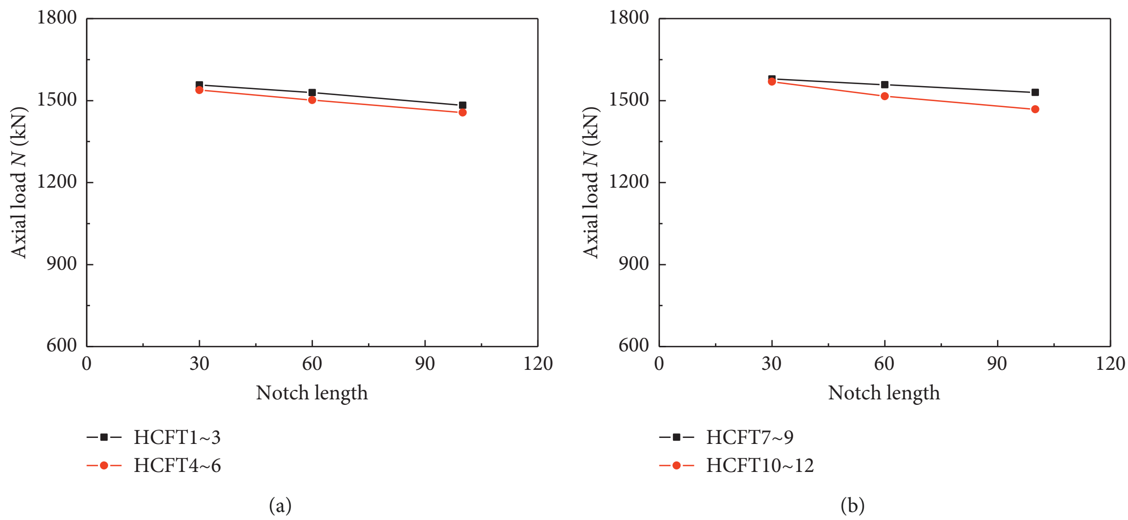

Figure 7: Influence of notch length on the ultimate strength of specimens. (a) Horizontal notch (HCFT1~HCFT6). (b) Vertical notch (HCFT7~HCFT12).

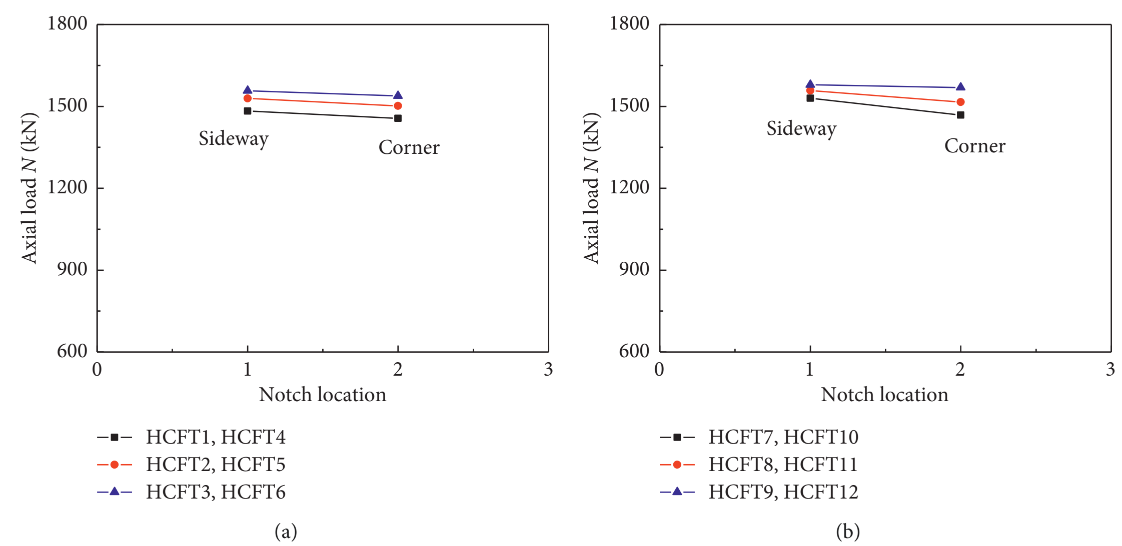

Figure 8: Influence of notch location on the ultimate strength of specimens. (a) Horizontal notch (HCFT1~HCFT6). (b) Vertical notch (HCFT7~HCFT12).

specimens, the carrying capacity of the specimens with a vertical notch is 2.0% larger than that of specimens with a horizontal notch. For corner-notched specimens, the carrying capacity of specimens with a vertical notch is 1.3% larger than that of specimens with a horizontal notch.

4. Calculation of the Ultimate Bearing Capacity of Notched CFST Columns

4.1. Bearing Strength. Ding et al. [17] proposed equation (1) to estimate the ultimate strength of notched hexagonal CFST columns.

$$N = f_c A_c (1 + K\Phi), \quad (1)$$

where A_c and A_s are the section area of concrete and steel tube, respectively; f_c is the compressive strength of concrete; f_{cu} is the strength of standard cube concrete; f_s is the yield strength of steel tube; Φ is a confinement index; and K is a coefficient ($K = 1.3$).

According to equation (1), the calculated ultimate bearing capacity of HCFT13 or HCFT13 is 1555 kN, and the ratio of measured to calculated values is 1.016. The results show that equation (1) can predict the ultimate strength of hexagonal CFST columns well. The equation was then applied as the basic computational formula for the ultimate strength of the notched specimens.

The slotting length, slotting orientation, and slotting location considerably affect the ultimate strength. Therefore, the ultimate strength of notched CFST columns can be expressed as

$$N = f_c A_c (1 + K_1 \Phi), \quad (2)$$

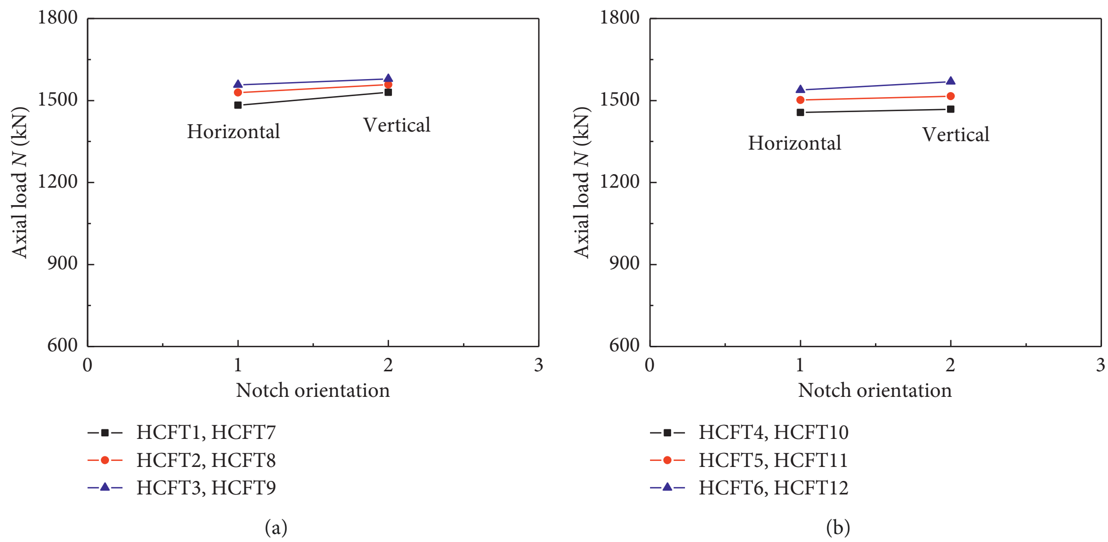

Figure 9: Influence of notch orientation on the ultimate strength of specimens. (a) Sideway notch (HCFT1~HCFT6). (b) Corner notch (HCFT7~HCFT12).

where K_1 is the reduction factor, which can be expressed as

$$K_1 = 1.3 - (0.6\beta_1 + 0.2\beta_2)\beta_3, \quad (3)$$

where β_1, β_2, and β_3 are parameters related to slotting length, slotting orientation, and slotting location, respectively, and expressed as

$$\beta_1 = \begin{cases} \dfrac{l}{S}, & \text{horizontal notch,} \\ \dfrac{b}{S}, & \text{vertical notch,} \end{cases}$$
$$\beta_2 = \begin{cases} \dfrac{b}{H}, & \text{horizontal notch,} \\ \dfrac{b}{S}, & \text{vertical notch,} \end{cases} \quad (4)$$
$$\beta_3 = \begin{cases} 1.3, & \text{sideway,} \\ 1, & \text{corner,} \end{cases}$$

where S, which is the outer girth of square steel pipe, is equal to 6 D.

Table 2 shows the calculated and experimental results for all the specimens. N_t and N_c are the test strength and calculated strength, respectively. The average N_t/N_c ratio is 1.004, with a coefficient of variation of 0.018 for spring element. Hence, equation (2) is acceptable.

4.2. Confining Effect. The notched steel pipe cannot exert sufficient restraint effect on the core concrete. This structure also has poor mechanical properties. Thus, estimating the restraint effect becomes essential. The ultimate strength of CSFT is the total of the contribution of the core concrete and steel pipe and the composite effect between the core concrete and steel pipe. It can be expressed as

$$N = A_s f_s + A_c f_c + F_s, \quad (5)$$

where F_s is the composite effect between the core concrete and steel pipe.

For notched columns, only a part of the steel pipe can carry the compression. Thus, the ultimate strength for a notched specimen can be defined as follows:

$$N_c = A_{se} f_s + A_c f_c + F_s. \quad (6)$$

For horizontal slotting, the effective area of the steel pipe (A_{se}) can be written as follows:

$$A_{se} = (D - 2t)t + (D - l - 2t)t + 2\ Dt. \quad (7)$$

For vertical slotting, the effective area of the steel pipe (A_{se}) can be written as follows:

$$A_{se} = (D - 2t)t + (D - b - 2t)t + 2\ Dt. \quad (8)$$

Hence, a confinement factor defined in equation (9) was applied to estimate the restraint effect of a notched steel pipe on the core concrete:

$$\lambda = \frac{F_s}{N_c}. \quad (9)$$

Table 2 shows the confinement factor for all the notched specimens. The results show the following: (1) The confinement factor of the horizontally notched specimen is greater than that of the vertically notched specimen. (2) The confinement factor of the sideway-notched specimen is smaller than the corner-notched ones. (3) For horizontally notched specimen, the longer the slotting, the greater is the confinement factor. In the vertically notched specimen, the confinement factor decreases when the duration of slotting increases.

Table 2: Confinement factor for all the notched specimens.

No.	A_{se} (mm^2)	A_c (mm^2)	f_s (MPa)	f_c (MPa)	N_c (kN)	F_s (kN)	λ
HCFT1	2000	25980	270	27.4	1468	215	0.147
HCFT2	2160	25980	270	27.4	1502	206	0.137
HCFT3	2280	25980	270	27.4	1527	199	0.130
HCFT4	2000	25980	270	27.4	1488	235	0.158
HCFT5	2160	25980	270	27.4	1514	218	0.144
HCFT6	2280	25980	270	27.4	1534	205	0.134
HCFT7	2360	25980	270	27.4	1519	169	0.111
HCFT8	2360	25980	270	27.4	1530	180	0.118
HCFT9	2360	25980	270	27.4	1539	188	0.122
HCFT10	2360	25980	270	27.4	1527	177	0.116
HCFT11	2360	25980	270	27.4	1536	186	0.121
HCFT12	2360	25980	270	27.4	1542	192	0.125
HCFT13	2400	25980	270	27.4	1555	194	0.125
HCFT14	2400	25980	270	27.4	1555	194	0.125

5. Conclusions

Fourteen CFST stub columns were included in the experiments, and notch length, notch location, and notch direction were considered. The effects of the structure-failure pattern were further investigated, and load-displacement curves were obtained. Finally, a method for calculating the ultimate strength of notched hexagonal CFST columns was established. The main conclusions are as follows.

(1) Compared with undamaged CFST columns under compression, the specimens showed failure modes that differ according to the slotting orientation. For horizontally notched specimens, the notch is closed under axial loading. For vertically notched ones, the slotting shows outward buckling phenomenon.

(2) The ultimate strength of notched CFST columns is less than that of intact CFST because the notched steel pipe cannot provide sufficient restraint on the core concrete. For notched hexagonal CFST column, the ultimate strength is less than those of undamaged ones. The experimental study illustrates that slotting length, slotting orientation, and slotting location considerably affect the ultimate strength of notched CFST columns.

(3) A formula proposed by Ding et al. [17] was used to estimate the ultimate strength of undamaged hexagonal CFST columns. On this basis, we establish an equation to predict the ultimate strength of notched hexagonal CFST columns. The calculation results are consistent with the experimental data.

Data Availability

All data used to support the findings of this study are included within the article. There are not any restrictions on data access.

Conflicts of Interest

The authors declare that they have no conflicts of interest.

Acknowledgments

This research work was financially supported by the Hunan Education Department Foundation Funded Project, Grant nos. 18B438 and 14C0217, the Project funded by China Postdoctoral Science Foundation, Grant no. 2018M632990, the Natural Science Foundation of Hunan Province, China, Grant nos. 2018JJ3021, 2018JJ2525, and 2019JJ20029, the National Key Research Program of China, Grant no. 2017YFC0703404, and the National Natural Science Foundation of China, Grant no. 51308548.

References

[1] L.-H. Han, C. Hou, and Q.-L. Wang, “Square concrete filled steel tubular (CFST) members under loading and chloride corrosion: Experiments,” *Journal of Constructional Steel Research*, vol. 71, no. 4, pp. 11–25, 2012.

[2] X. Zhou, G. Cheng, J. Liu, D. Gan, and Y. Frank Chen, “Behavior of circular tubed-RC column to RC beam connections under axial compression,” *Journal of Constructional Steel Research*, vol. 130, no. 3, pp. 96–108, 2017.

[3] C. Tian, C. Xiao, T. Chen, and X. Fu, “Experimental study on through-beam connection system for concrete filled steel tube column-RC beam,” *Steel and Composite Structures*, vol. 16, no. 2, pp. 187–201, 2014.

[4] J. Pan, P. Wang, Y. Zheng, Z. Wang, and D. Liu, “An analytical study of square CFT columns in bracing connection subjected to axial loading,” *Advances in Civil Engineering*, vol. 2018, Article ID 8618937, 15 pages, 2018.

[5] R. Montuori and V. Piluso, “Analysis and modelling of CFT members: moment curvature analysis,” *Thin-Walled Structures*, vol. 86, no. 1, pp. 157–166, 2015.

[6] A. A. Nia, K. F. Nejad, H. Badnava, and H. R. Farhoudi, “Effects of buckling initiators on mechanical behavior of thin-walled square tubes subjected to oblique loading,” *Thin-Walled Structures*, vol. 59, no. 11, pp. 87–96, 2012.

[7] Z. Sadovský, J. Kriváček, V. Ivančo, and A. Ďuricová, “Computational modelling of geometric imperfections and buckling strength of cold-formed steel,” *Journal of Constructional Steel Research*, vol. 78, no. 12, pp. 1–7, 2012.

[8] X.-W. Zhang, H. Su, and T.-X. Yu, “Energy absorption of an axially crushed square tube with a buckling initiator,” *International Journal of Impact Engineering*, vol. 36, no. 3, pp. 402–417, 2009.

[9] A. A. Nia, H. Badnava, and K. F. Nejad, "An experimental investigation on crack effect on the mechanical behavior and energy absorption of thin-walled tubes," *Materials & Design*, vol. 32, no. 6, pp. 3594–3607, 2011.

[10] X. Chang, L. Fu, H.-B. Zhao, and Y.-B. Zhang, "Behaviors of axially loaded circular concrete-filled steel tube (CFT) stub columns with notch in steel tubes," *Thin-Walled Structures*, vol. 73, no. 12, pp. 273–280, 2013.

[11] F.-X. Ding, L. Fu, and Z.-W. Yu, "Behaviors of axially loaded square concrete-filled steel tube (CFST) Stub columns with notch in steel tube," *Thin-Walled Structures*, vol. 115, no. 6, pp. 196–204, 2017.

[12] Y. Liu and B. Young, "Buckling of stainless steel square hollow section compression members," *Journal of Constructional Steel Research*, vol. 59, no. 2, pp. 165–177, 2003.

[13] Z.-P. Chen, Y.-L. Chen, and M. Zhong, "Experimental study on axial compression capacity of concrete-filled square steel tubular columns with opening hole damage," *Building Structure*, vol. 44, no. 9, pp. 9–14, 2014, in Chinese.

[14] Z.-P. Chen, Y.-L. Chen, and M. Zhon, "Experimental study on mechanical properties of concrete-filled opening hole damaged steel tubular members," *Industrial Construction*, vol. 43, no. 2, pp. 121–127, 2013.

[15] F.-X. Ding, Z. Li, S. Cheng, and Z.-w. Yu, "Composite action of octagonal concrete-filled steel tubular stub columns under axial loading," *Thin-Walled Structures*, vol. 107, no. 11, pp. 453–461, 2016.

[16] W. Xu, L.-H. Han, and W. Li, "Performance of hexagonal CFST members under axial compression and bending," *Journal of Constructional Steel Research*, vol. 24, no. 3, pp. 309–322, 2017.

[17] F.-X. Ding, Z. Li, S. Cheng, and Z.-w. Yu, "Composite action of hexagonal concrete-filled steel tubular stub columns under axial loading," *Thin-Walled Structures*, vol. 107, no. 11, pp. 502–513, 2016.

[18] M. F. Hassanein, V. I. Patel, and M. Bock, "Behaviour and design of hexagonal concrete-filled steel tubular short columns under axial compression," *Engineering Structures*, vol. 153, no. 12, pp. 732–748, 2017.

[19] B. Evirgen, A. Tuncan, and K. Taskin, "Structural behavior of concrete filled steel tubular sections (CFT/CFSt) under axial compression," *Thin-Walled Structures*, vol. 80, no. 7, pp. 46–56, 2014.